Molecular structure and magnetic properties of copper(II), manganese(II) and iron(II) croconate tri-hydrate

Andrea Cornia, Antonio C. Fabretti* and Aleardo Giusti
Dipartimento di Chimica dell'Università, via G. Campi 183, 41100 Modena (Italy)

Fabrizio Ferraro and Dante Gatteschi*
Dipartimento di Chimica dell'Università, via Maragliano 75, 50144 Florence (Italy)

(Received January 21, 1993)

Abstract

The compounds $M^{II}C_5O_5 \cdot 3H_2O$ with M = Cu (**I**), Mn (**II**), Fe (**III**), were prepared and characterized by means of structural and magnetic measurements. The crystals are orthorhombic, space group *Pbca*, with $a = 11.770(2)$, $b = 8.085(2)$, $c = 15.571(2)$ Å for **I**, $a = 12.063(3)$, $b = 8.213(2)$, $c = 15.652(3)$ Å for **II**, $a = 11.999(2)$, $b = 8.158(1)$, $c = 15.536(4)$ Å for **III**; $Z = 8$. The previously reported structures of **I** and **II**, refined in this work, and the novel structure of **III** were solved by direct methods and least-squares refinement of structural parameters led to conventional R factors of 0.029, 0.025 and 0.025 for **I**, **II** and **III**, respectively. The overall structure is similar for the three compounds and consists of infinite one-dimensional chains of metal ions bridged by croconate ligands acting in a monodentate and bidentate fashion. The magnetic properties of **I**, **II** and **III** are reported and discussed on the basis of intrachain and interchain exchange couplings and, for **III**, of single-ion axial zero-field splitting contributions. Weak antiferromagnetic intrachain interactions via the croconate dianion ($J = 0.99(3)$, 0.22(1) and $\leqslant 0.54$ cm^{-1} for **I**, **II** and **III**, respectively) appear to be responsible of most of the observed magnetic behavior.

Introduction

Monocyclic aromatic oxocarbon dianions $[C_nO_n]^{2-}$, i.e. deltate ($n = 3$), squarate (4), croconate (5), rhodizonate (6), etc., have been extensively studied in recent years [1, 2] and their coordination chemistry is a current subject of research. Several compounds have been reported in which transition metal and f element ions are bound either to squarate (Cr(III) [3, 4], Mn(II) [3, 5, 6], Fe(II) [3], Fe(III) [3, 7], Co(II) [3], Ni(II) [3, 8–10], Cu(II) [3, 11–15], polyoxomolybdate(VI) [16–18], Pt(II) [19–21] and rare-earth [22] cations) or to croconate anions (Cr(III) [23], Mn(II) [23–25], Fe(II) [23], Fe(III) [23], Co(II) [23], Ni(II) [23], Cu(II) [23, 26–29], MoO_2(VI) [30], rare-earth [31] cations, Th(IV) and UO_2(VI) [32]).

We are interested in the magnetic properties of compounds in which transition metal ions, bridged by monocyclic oxocarbon dianions, are arranged in extended structures. At the moment, only a few such compounds with either squarate [8–10, 13, 15] or croconate [25] as ligand have been magnetically characterized. In particular we have focused our attention on compounds of general formula $M^{II}C_5O_5 \cdot 3H_2O$, whose structures consist of chains in which the croconate anions bridge two metal ions by using three oxygen donor atoms in a monodentate and bidentate fashion. For $CuC_5O_5 \cdot 3H_2O$ (**I**) and $MnC_5O_5 \cdot 3H_2O$ (**II**), old dated structural parameters are available [24, 26], while up to now for the other members of the series no detailed X-ray analysis has been carried out.

We present here the results of the structural refinement of **I** and **II**, which was performed with the aim of having accurate structural data for discussing their magnetic properties, together with the novel X-ray structure determination for $FeC_5O_5 \cdot 3H_2O$ (**III**). We also present the magnetic behavior of **I**, **II** and **III** in the range 2.2–280 K and the analysis of the exchange pathways connecting the transition metal ions. Up to now, the magnetic properties have been reported for the manganese compound (**II**) only [25].

Experimental

Synthesis

All chemicals were reagent grade and used as received. The complexes were obtained by mixing the metal

*Authors to whom correspondence should be addressed.

0020-1693/93/$6.00

chloride (1 mmol) in 8 ml H_2O with potassium croconate (1 mmol) in 20 ml H_2O [3]. Brown crystals were obtained for all the compounds. *Anal.* Calc. for $CuC_5O_5 \cdot 3H_2O$ (**I**): C, 23.31; H, 2.35. Found: C, 23.36; H, 2.37%. Calc. for $MnC_5O_5 \cdot 3H_2O$ (**II**): C, 24.12; H, 2.43. Found: C, 24.16; H, 2.57%. Calc. for $FeC_5O_5 \cdot 3H_2O$ (**III**): C, 24.03; H, 2.42; Found: C, 24.06; H, 2.45%.

Crystal data

Brown crystals consisting of well shaped individuals defined by three pairs of pinacoids were obtained by slow crystallization of the reaction mixture. X-ray data were collected at room temperature on an Enraf-Nonius CAD 4 diffractometer with Mo Kα radiation. During the measurements the crystal decay was tested by detecting the intensity of standard reference reflections at time intervals. The crystal parameters and information on the data collection and reduction are given in Table 1. All the data were corrected for Lorentz and polarization effects, and an empirical absorption correction, based on the Ψ scan, was applied [33].

The structures were solved by direct methods, which provided positions of the metal ions; all the remaining non-hydrogen atoms were located by subsequent difference-Fourier syntheses. The refinement was carried out by least-squares calculations including the atomic coordinates and anisotropic thermal parameters of the non-hydrogen atoms. The hydrogen atoms were treated as fixed contributors at found positions, assuming a temperature factor 1 Å^2 greater than that of the attached oxygen atoms. Complex neutral-atom scattering factors [34] were employed throughout; major calculations were carried out on a Vax 6210 computer, using the SHELX 76 [35] program package and the ORTEP [36] plotting program. The refined non-hydrogen atomic coordinates are listed in Table 2.

Magnetic and EPR measurements

Magnetic susceptibilities of powdered samples were measured in the temperature range 2.2–280 K in a field of 2 T for **I** and **III** and 1 T for **II** by using a Métronique Ingéniérie MS03 SQUID magnetometer. Diamagnetic corrections were estimated from Pascal's constants. For **III**, magnetization data were obtained by using the magnetometer mentioned above, at $T = 2.3$ and 4.4 K in the field range 0–7 T.

EPR spectra of powdered samples were obtained with a Varian E9 spectrometer at X-band frequency, equipped with an Oxford Instruments ESR9 liquid helium continuous flow cryostat.

Results and discussion

Crystal structures

The relevant interatomic bond distances and bond angles for the three compounds are given in Table 3. See also 'Supplementary material'. The structures of $CuC_5O_5 \cdot 3H_2O$ (**I**) and $MnC_5O_5 \cdot 3H_2O$ (**II**), refined in this work, were described by Glick *et al.* [26, 24]. The agreement factors of our refinement are much smaller than those of the previous refinements. However no significant variation in the crystal structure is observed. Both structures consist of infinite chains with each metal(II) coordinated to two adjacent oxygens of one croconate ring and to a single oxygen of a second croconate ring such that only two non-adjacent oxygens per croconate ring are not coordinated. The asymmetric repeating unit comprising one metal(II), one croconate ring and three water molecules is shown in Fig. 1. The zig-zag chains are parallel to the *c* axis. The six-coordinated metal(II) is surrounded by three croconate oxygens and three waters at the corners of a distorted octahedron.

The structure of $FeC_5O_5 \cdot 3H_2O$ (**III**) is analogous to the previous ones. The average metal–oxygen distance is 2.137 Å, to be compared to 2.193 Å for the manganese(II) and to 2.104 Å for the copper(II) compound, in agreement with the trend in the ionic radii of the metals. The Fe–O(1) and Fe–O(2) distances with the chelating oxygens of the croconate are markedly different, the asymmetry being intermediate between those observed in **I** and **II**. The Fe–O(3) distance corresponding to the third croconate oxygen is comparable to Fe–O(1), analogously to the manganese complex. In **I** the Cu–O(3) distance is long and in fact O(2)–Cu–O(3) corresponds to the elongation axis of the copper octahedral environment, while in **II** and **III** the bond anisotropy is much smaller and the distortion is not axial.

Magnetic and EPR data

EPR spectra of polycrystalline powders of $CuC_5O_5 \cdot 3H_2O$ (**I**) recorded at room temperature and 4.2 K, respectively, are shown in Fig. 2. The spectra are axial and the observed *g* values are $g_{\parallel}^{obs} = 2.12$ and $g_{\perp}^{obs} = 2.22$ at room temperature, $g_{\parallel}^{obs} = 2.085$ and $g_{\perp}^{obs} = 2.25$ at 4.2 K.

$MnC_5O_5 \cdot 3H_2O$ (**II**) EPR spectra show a single line centered at $g \cong 2$ at both room and liquid helium temperature. The peak to peak linewidth ΔH is 160 G at 293 K, much smaller than 800 G reported by Deguenon *et al.* [25]; it increases at low temperature: its values are $\Delta H = 235$ G at 16 K and 370 G at 4.2 K.

$FeC_5O_5 \cdot 3H_2O$ (**III**) does not show any detectable EPR signal in the temperature range explored.

TABLE 1. X-ray crystallography

Crystal parameters[a] *at 20 °C*			
Formula	$C_5O_8H_6Cu$	$C_5O_8H_6Mn$	$C_5O_8H_6Fe$
Molecular weight	257.644	249.036	249.945
Crystal system	orthorhombic	orthorhombic	orthorhombic
Space group	*Pbca* (No. 61)	*Pbca* (No. 61)	*Pbca* (No. 61)
a (Å)	11.770(2)	12.063(3)	11.999(2)
b (Å)	8.085(2)	8.213(2)	8.158(1)
c (Å)	15.571(2)	15 652(3)	15.536(4)
V (Å^3)	1481.7(5)	1550.7(6)	1521.0(6)
Z	8	8	8
D_c (D_f) (g cm^{-3})	2.31 (2.29)	2.13 (2.15)	2.18(2.16)
F(000)	1032	1000	1008
Data collection			
Radiation[b]	Mo Kα	Mo Kα	Mo Kα
Reflection measured	$\pm h$, $+k$, $+l$	$\pm h$, $+k$, $+l$	$\pm h$, $+k$, $+l$
Scan type	ω–2θ	ω–2θ	ω–2θ
Range (°)	2–30	2–28	2–30
Scan width (°)	$0.55+0.35\ \tan\theta$	$0.55+0\ 35\ \tan\theta$	$0.55+0.35\ \tan\theta$
Scan speed limits (° min^{-1})	0.91–5.49	0.87–5 49	0.91–5 49
Standard reflections	2 every 3 h (no changes)	2 every 3 h (no changes)	2 every 3 h (no changes)
Collected reflections	4668	4124	4775
Observed reflections	1963 with $I \geqslant 3\sigma(I)$	2441 with $I \geqslant 3\sigma(I)$	2088 with $I \geqslant 3\sigma(I)$
Independent reflections	1177 ($R_{merge}=0.022$)	1789 ($R_{merge}=0.029$)	1456 ($R_{merge}=0.025$)
Crystal size (mm)	$0\ 25\times0.25\times0.20$	$0.20\times0.20\times0.20$	$0\ 20\times0.25\times0.20$
μ(Mo Kα) (cm^{-1})	22.7	16.2	19.0
Absorption correction[c]	$0.99 > T_{factor} > 0.95$	$0\ 99 > T_{factor} > 0.95$	$0.99 > T_{factor} > 0.95$
Structure determination			
Structure solution	direct methods[d]	direct methods[d]	direct methods[d]
Structure refinement	full-matrix least-squares[e]	full-matrix least-squares[e]	full-matrix least-squares[e]
Non-H atoms	anisotropic	anisotropic	anisotropic
H atoms	fixed contributors[f]	fixed contributors[f]	fixed contributors[f]
No. varied parameters	127	127	127
R	0.029	0.025	0.025
R_w	0.026	0 025	0.027
w	$1.1/[\sigma^2(F_o)+0.000100F_o^2]$	$1.2/[\sigma^2(F_o)+0\ 000100F_o^2]$	$1\ 5/[\sigma^2(F_o)+0.000100F_o^2]$
$\Delta\rho$: min., max. (e Å^{-3})	−0.46, +0.48	−0.38, +0.41	−0.44, +0.46

[a]By least-squares refinement on setting angles of 25 automatically centered reflections ($\lambda=0.71069$ Å). [b]Graphite monochromated; $\lambda=0.71069$ Å. [c]Based on empirical Ψ scan. [d]SHELX86 program. [e]SHELX76 program. [f]H atoms located in ΔF maps, refined isotropically through some least-squares cycles, and then held as fixed contributors

$\chi_m T$ versus T curves for **I** and **II** are shown in Fig. 3, and for **III** in Fig. 4. For the three compounds $\chi_m T$ is approximately constant down to about 20 K for **I**, 50 K for **II** and 60 K for **III**. The room temperature values $\chi_m T = 0.45$, 4.1 and 3.72 emu K mol^{-1} are close to those expected for $S = 1/2$, 5/2, 2 uncorrelated spins, respectively. $\chi_m T$ decreases on decreasing temperature, reaching the values 0.32 emu K mol^{-1} at 2.2 K for **I**, 2.40 emu K mol^{-1} at 3.3 K for **II** and 1.37 emu K mol^{-1} at 2.8 K for **III**. The susceptibilities χ_m do not show any maximum in the temperature range explored for the three compounds.

The magnetization versus H curves at $T = 2.3$ and 4.4 K for **III** are reported in Fig. 5. For $H < 2$ T a linear dependence of magnetization versus field is observed. At the highest fields explored, the magnetization is fairly independent of the field and its value at $H = 7$ T is 19 800 emu G mol^{-1}. ($\equiv 3.54$ μ_B). However, complete saturation is not achieved.

EPR spectra are sensitive to the magnetic exchange interactions between the paramagnetic centers in the system [37], and the spectra of **I** clearly show these effects. In fact, in the absence of exchange $g_{\parallel}$ is expected to be larger than $g_{\perp}$ for Cu(II) spins in the tetragonally elongated environment [38], while the reverse is found for **I**. This fact can be explained on the basis of the structure of the compound. The axis of tetragonal elongation for copper(II), O(2)–Cu–O(3), lies approximately in the *bc* plane and forms an angle of about 45° with *c*, the direction of the axis of the chain –(–Cu–croconate–)$_n$–. In the chain, the axis of elongation of two adjacent Cu(II) ions, related by a glide plane b_c, are therefore almost perpendicular to each other [26]. In the presence of intrachain and interchain

TABLE 2 Final positional parameters of $MC_5O_5\ 3H_2O$

Atom	x	y	z
Cu	0.12772(4)	0.10616(4)	0.18837(2)
O(1)	0.1343(3)	0.2784(3)	0 2785(1)
O(2)	0.1179(2)	−0.0615(3)	0.3082(2)
O(3)	0.1396(3)	0.3068(3)	0.0810(1)
O(4)	0.1151(2)	−0.0783(3)	0.1076(1)
O(5)	−0.0420(2)	0.1314(3)	0.1823(2)
O(6)	0.3004(2)	0.0992(3)	0.1799(2)
O(7)	0.1195(2)	0 6245(3)	−0.0024(2)
O(8)	0 1314(2)	0.4553(3)	0.4474(1)
C(1)	0.1309(3)	0.2164(4)	0.3536(2)
C(2)	0 1238(3)	0.0409(4)	0 3681(2)
C(3)	0.1245(3)	0.4911(4)	−0.0394(2)
C(4)	0.1333(3)	0.3264(4)	0.0021(2)
C(5)	0.1323(3)	0.1977(4)	−0.0648(2)
Mn	0.12367(2)	0.11598(3)	0.18594(2)
O(1)	0.1347(1)	0.3055(2)	0.2848(1)
O(2)	0.1151(1)	−0.0287(2)	0.3082(1)
O(3)	0.1372(1)	0.2943(2)	0.0841(1)
O(4)	0.1095(1)	−0.1006(2)	0.1136(1)
O(5)	−0.0559(1)	0.1525(1)	0.1779(1)
O(6)	0.3080(1)	0.0993(2)	0 1781(1)
O(7)	0.1195(1)	0.6020(2)	−0.0039(1)
O(8)	0.1329(1)	0 4717(2)	0.4543(1)
C(1)	0.1313(2)	0.2421(2)	0.3576(1)
C(2)	0.1230(2)	0.0685(2)	0.3699(1)
C(3)	0 1240(2)	0.4687(2)	−0 0388(1)
C(4)	0.1324(2)	0.3088(2)	0.0048(1)
C(5)	0.1327(2)	0.1781(2)	−0.0596(1)
Fe	0.12599(3)	0.11815(3)	0.18563(2)
O(1)	0.1358(2)	0.3071(2)	0.2803(1)
O(2)	0.1163(1)	−0.0272(2)	0.30486(9)
O(3)	0 1371(2)	0.2899(2)	0.08301(9)
O(4)	0.1111(1)	−0.0915(2)	0.1132(1)
O(5)	−0.0503(1)	0.1543(2)	0.1821(1)
O(6)	0.3058(1)	0.1035(2)	0.1758(1)
O(7)	0.1201(2)	0.5993(2)	−0.0043(1)
O(8)	0.1328(1)	0.4768(2)	0.4512(1)
C(1)	0.1318(2)	0.2443(3)	0.3545(1)
C(2)	0.1233(2)	0.0700(2)	0.3673(1)
C(3)	0.1245(2)	0 4652(2)	−0.0406(1)
C(4)	0.1320(2)	0.3049(3)	0.0033(1)
C(5)	0.1330(2)	0.1744(3)	−0.0620(1)

exchange interactions, the observed $g_{\parallel,\perp}{}^{obs}$ values are therefore related to the single ion $g_{\parallel,\perp}{}^{Cu}$ values according to

$$g_{\parallel}{}^{obs}=g_{\perp}{}^{Cu} \qquad g_{\perp}{}^{obs}=(g_{\parallel}{}^{Cu}+g_{\perp}{}^{Cu})/2$$

the directions of the principal components of the $\mathbf{g}^{obs}$ tensor being along the *a* axis and in the *bc* plane, respectively. From the room temperature experimental $g_{\parallel,\perp}{}^{obs}$ values we obtain for the single Cu(II) ion the values $g_{\parallel}{}^{Cu}=2.32$ and $g_{\perp}{}^{Cu}=2.12$, which agree with those expected for Cu(II) spins in the tetragonally elongated environment of six oxygen donors. The small difference between the *g* values observed at room and liquid helium temperature can be attributed to minor structural variations of the Cu(II) coordination site.

On the basis of the similar structure of **I**, **II** and **III**, exchange interactions between the paramagnetic centers are expected not only for **I**, but also for **II** and **III**. Therefore, a correct interpretation of the magnetic data of the title compounds would require the consideration of the intrachain exchange interactions between the metal spins via the croconate bridge and of the interchain interactions via the $M–OH_2\cdots OH_2–M$ and $M–OH_2\cdots O(C_5O_5)–M$ paths. The decrease of $\chi_m T$ at low temperature and the absence of maxima in the χ_m versus T curves for the three compounds in the range of temperature explored indicate that the result of this network of interactions is an antiferromagnetic coupling between the spins with an effective coupling constant J smaller than about 2 cm^{-1}.

The discrimination between intra- and interchain couplings is not easy. Magnetic susceptibilities data for $MnC_5O_5\cdot 3H_2O$ (**II**) were reproduced [25] by introducing a temperature Θ [39] in the classical spin Heisenberg chain model [40]. The result obtained was the absence of intrachain interactions via the croconate bridge, while the interchain interactions were found to yield $\Theta=3$ K ($\equiv 2.09$ cm^{-1}). However the introduction of the parameter Θ to account for the interchain interactions seems rather doubtful. Besides, exchange couplings as large as 9.63 cm^{-1} have been found to be transmitted through the croconate ligand in a Cu(II) dimer [27].

To our knowledge, no other direct experimental finding for the values of the interchain exchange interactions transmitted through paths like those in the text compounds is reported. However, there are some indirect indications about the values for such interactions. In fact, exchange interactions transmitted via H_2O molecules were found to be associated to the transition to magnetically ordered phases in several low dimensional compounds [41, 42]. In these cases, a good estimation of the interchain exchange interactions j is obtained from both the values of the intrachain coupling constant J and the transition temperature T_c ($T_c=(2J/k_B)S(S+1)\ (j/J)^{1/2}$ [43]. In the one-dimensional compounds $Mn^{II}M^{II}(EDTA)\cdot 6H_2O_2$ with M=Cu, Ni, the interchain coupling constant was estimated to be very small and of the order of 10^{-3} cm^{-1} [42]. The intrachain exchange interactions in these compounds are transmitted via paths $M–OH_2\cdots O(EDTA)–Mn$ and $M–OH_2\cdots H_2O–M$ [44]. These paths are structurally very similar to those observed in the title compounds. Therefore we think that the values of the interchain coupling constants are of the same order in the two cases and in the fitting of the magnetic susceptibilities we neglect the interchain exchange interactions, too weak to cause the decrease of the $\chi_m T$ product observed for the three compounds.

We reproduced the data of χT versus T for **I** and **II** describing the two compounds as Heisenberg chains with the Hamiltonian

TABLE 3. Bond distances (Å) and bond angles (°) with e.s.d.s in parentheses of $MC_5O_5\ 3H_2O$

	Cu	Mn	Fe		Cu	Mn	Fe
M–O(1)	1.978(2)	2.199(1)	2.134(2)	M–O(2)	2.309(2)	2.254(1)	2.202(2)
M–O(3)	2 334(2)	2.172(1)	2.127(2)	M–O(4)	1.957(2)	2.115(1)	2.055(2)
M–O(5)	2.011(2)	2.191(1)	2.137(2)	M–O(6)	2 037(2)	2.228(1)	2.166(2)
O(1)–M–O(2)	80.9(1)	77.3(1)	79.2(1)	O(1)–M–O(3)	91.0(1)	92 0(1)	92.1(1)
O(2)–M–O(3)	171.9(1)	169.2(1)	171.3(1)	O(1)–M–O(4)	174 5(1)	167.7(1)	169.5(1)
O(2)–M–O(4)	93 9(1)	90.5(1)	90.5(1)	O(3)–M–O(4)	94 2(1)	100 3(1)	98.3(1)
O(1)–M–O(5)	90.0(1)	90.1(1)	88.4(1)	O(2)–M–O(5)	92.7(1)	94.3(1)	92.5(1)
O(3)–M–O(5)	87.4(1)	86.6(1)	87.2(1)	O(4)–M–O(5)	88.4(1)	90 3(1)	90.9(1)
O(1)–M–O(6)	91.5(1)	91.2(1)	91.9(1)	O(2)–M–O(6)	94.9(1)	93.4(1)	94.8(1)
O(3)–M–O(6)	85.0(1)	85.8(1)	85.5(1)	O(4)–M–O(6)	90.7(1)	90.0(1)	90.1(1)
O(5)–M–O(6)	172.3(1)	172.3(1)	172.7(1)				

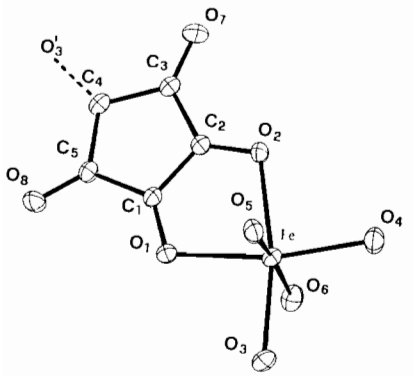

Fig. 1. ORTEP drawing of $FeC_5O_5 \cdot 3H_2O$ (**III**) with the adopted numbering scheme. The hydrogen atoms are not represented for clarity.

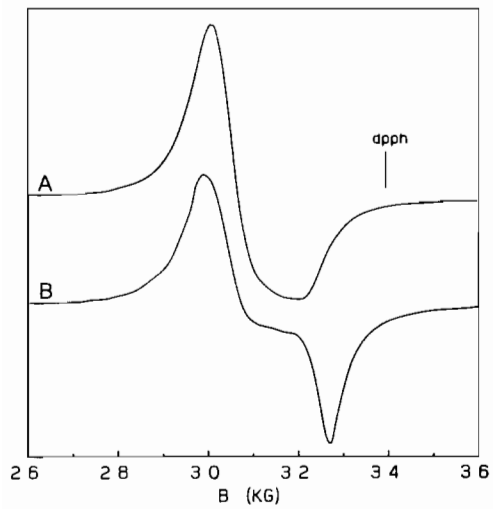

Fig. 2. Powdered sample EPR spectra of $CuC_5O_5 \cdot 3H_2O$ (**I**) at room temperature (A) and 4.2 K (B). The intensities are arbitrary.

$$\mathscr{H} = J \sum_{i=1}^{N-1} S_i S_{i+1} \qquad (1)$$

where J is the coupling constant via the croconate ligand. For **I**, the fitting of $\chi_m T$ versus T curve was

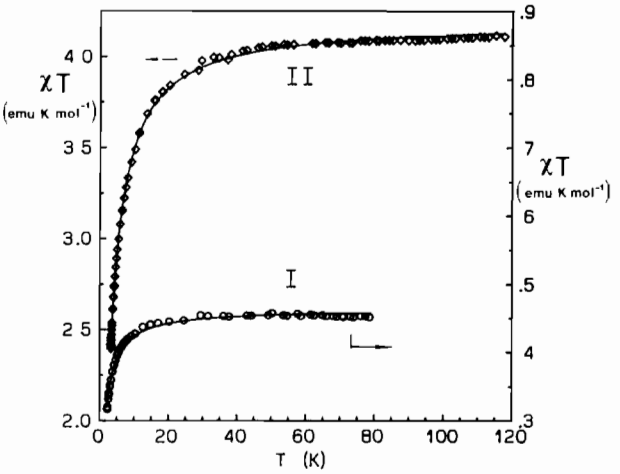

Fig. 3. $\chi_m T$ vs. T for $CuC_5O_5 \cdot 3H_2O$ ((**I**) and $MnC_5O_5 \cdot 3H_2O$ (**II**). The solid lines represent the least-squares best fits (see text).

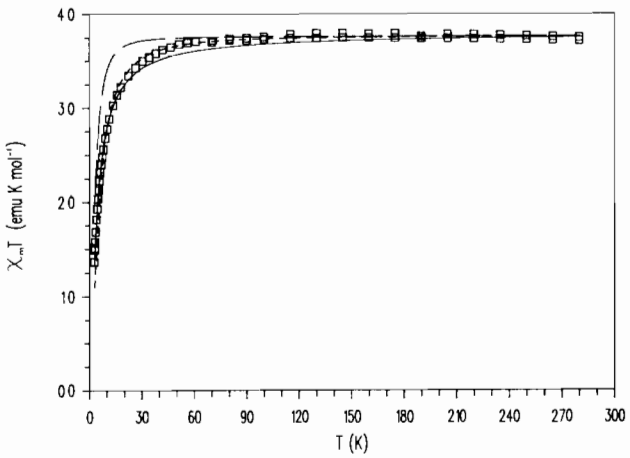

Fig. 4. $\chi_m T$ vs. T for $FeC_5O_5\ 3H_2O$ (**III**). The curves represent: (i) the result of the least-squares fitting in the limit case of Hamiltonian (1) (——); (ii) the values calculated in the limit of Hamiltonian (4) with $D = 12.5$ (– – – –) and 4.0 (– · –) cm^{-1}.

performed by using the Bonner–Fisher numerical formula for the quantum antiferromagnetic chain formed by $S = 1/2$ spins [45]:

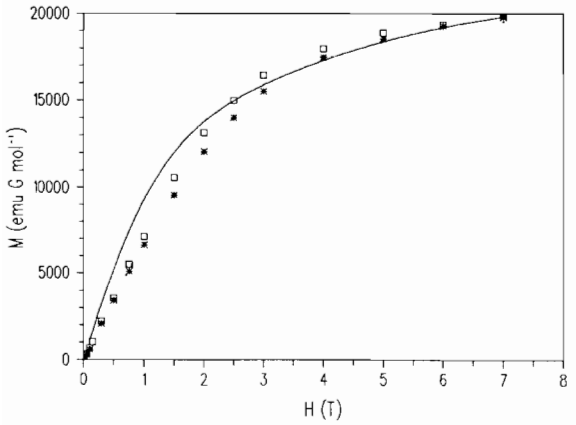

Fig. 5. Magnetization vs. H data for $FeC_5O_5 \cdot 3H_2O$ (**III**) at $T=2.3$ (□) and 4.4 (*) K. The curves are calculated with $D=4.0$ cm^{-1} at both 2.3 (——) and 4.4 (· · ·) K.

$$\chi_m T = (Ng^2\mu_B^2/k_B)[(A + Bx + Cx^2)/(1 + Dx + Ex^2 + Fx^3)] \quad (2)$$

with $x = J/2k_BT$ and A–F numerical coefficients. For **II** the classical spin approach was followed [40]:

$$\chi_m T = (Ng^2\mu_B^2/3k_B)S(S+1)[(1+u)/(1-u)] \quad (3)$$

with $u = \coth K - 1/K$ and $K = JS(S+1)/k_BT$. The results of the least-squares fitting procedure were for **I**: $J=0.99(3)$ cm^{-1}, with $g=2.18$ and $R=8.03\times10^{-5}$; for **II**: $J=0.22(1)$ cm^{-1}, with $g=1.96$ and $R=2.69\times10^{-5}$* (Fig. 3).

For the Fe(II) compound (**III**) the situation is more complicated, since the energy spectrum associated to the complete Hamiltonian, containing both the exchange contributions and Fe(II) single-ion zero-field splitting, is not available. Therefore we tried to reproduce the $\chi_m T$ data in the two limit cases of either an exchange coupled spin chain or an isolated spin with axial zero-field splitting contributions. In the first limit case of exchange coupled $S=2$ spins the above mentioned classical approach was followed. The result of the least-squares fitting of $\chi_m T$ versus T for **III** is $J=0.54$ cm^{-1}, with $g=2.25$ and $R=2.5\times10^{-4}$* (Fig 4). On the other hand, when taking into account single-ion axial zero-field splitting only, we described the system through the Hamiltonian.

$$\mathcal{H} = D[(S^z)^2 - 1/3S(S+1)] + g\mu_B SH \quad (4)$$

The temperature dependence of $\chi_m T$, where $\chi_m = 1/3(\chi_\parallel + 2\chi_\perp)$, could be resonably well reproduced by using a D value of 12.5 cm^{-1}, with g fixed at 2.23 in order to fit the high temperature data (Fig. 4). This quite large, positive D value agrees with what was found for octahedral Fe(II) ions [46]; however the study of the low temperature magnetization curves is necessary to get more precise estimations of the D value in **III**. Indeed, a much lower value $D \cong 4.0$ cm^{-1} is required to reproduce the magnetization curves in the high field range ($H < 2T$), where the effects of lower interactions, such as intra- and interchain exchange couplings and not axial zero-field splitting terms, are negligible (Fig. 5). The $\chi_m T$ versus T curve calculated with the value $D=4.0$ cm^{-1} is shown in Fig. 4. For temperatures lower than 50 K it is quite above the experimental values, indicating the presence in the system of meaningful exchange interactions, not much lower than $J=0.54$ cm^{-1} calculated in the limit of Hamiltonian (1), and attributable to the intrachain couplings.

As a summary, we have found that the croconate ligand in the $M^{II}(C_5O_5)\cdot 3H_2O$ series is able to transmit an antiferromagnetic exchange coupling between the spins of M^{II} paramagnetic ions, although weak. It is interesting to compare the value of the exchange coupling constants found here for the title compounds with the values reported for other compounds in which the croconate anions act as bridges between M^{II} ions. The antiferromagnetic coupling transmitted via the croconate ligand in **I** is much weaker than observed ($J=9.63$ cm^{-1}) in the Cu(II) dimer $[Cu_2(bpca)_2C_5O_5]\cdot 3H_2O$, where bpca is the bis(2-pyridylcarbonyl)amide anion [27]. The origin of the different J values found in the two compounds can be attributed to the different bridging geometries of the croconate dianion. In $[Cu_2(bpca)_2C_5O_5]\cdot 3H_2O$ the croconate dianion acts as a bis-bidentate ligand, while in **I** it is mono-bidentate as shown below.

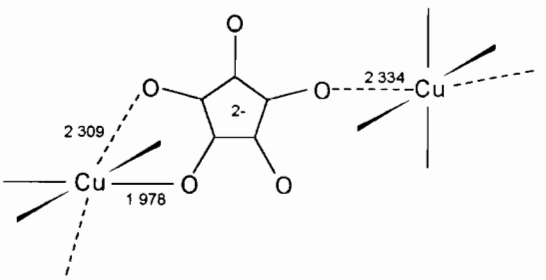

$CuC_5O_5\cdot 3H_2O$

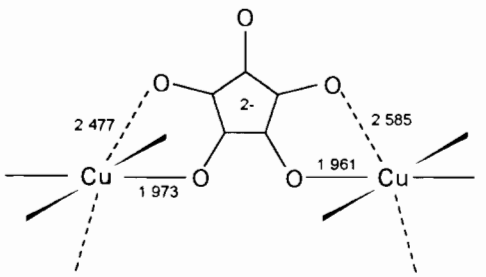

$[Cu_2(bpca)_2\,C_5O_5]\cdot 3H_2O$

*$R = \Sigma(\chi_{obs}T - \chi_{calc}T)^2/\Sigma(\chi_{obs}T)^2$.

The unpaired electron in copper(II) is in a $d_{x^2-y^2}$ orbital. In **I** the $d_{x^2-y^2}$ orbital of one copper(II) interacts strongly with the croconate oxygen at 1.978 Å, but the interaction with the $d_{x^2-y^2}$ of the second copper(II) ion must be weak because the corresponding oxygen atom is an axial site connected only through a long bond. In $[Cu_2(bpca)_2C_5O_5]\cdot 3H_2O$ on the other hand, both copper(II) ions are bound to two oxygen atoms with short bonds involving the $d_{x^2-y^2}$ orbitals. Therefore the much larger J value observed in the latter case is justified on structural grounds.

Another noteworth feature is the small variation of the coupling constant J on changing the metal ion in the series. In isostructural transition metal compounds, the coupling constant between like spins is expected to vary approximately as $1/n^2$, where n is the number of d electrons [47]. However, in the Cu(II), Fe(II) and Mn(II) croconates the coupling constants $J = 0.99$, $\leqslant 0.54$ and 0.22 do not scale as 1:1/16:1/25. In particular the coupling constant in $CuC_5O_5\cdot 3H_2O$ is much smaller than expected, relative to the other compounds. This may depend on the tetragonal distortion of copper(II) ions in **I**, which depress the antiferromagnetic couplings, due to the long metal–oxygen distances.

Supplementary material

Anisotropic thermal parameters (Table 1S, 1 page); positional and thermal parameters for hydrogen atoms (Table 2S, 1 page); bond distances and angles involving hydrogen atoms (Table 3S, 1 page); additional bond distances and angles involving non-hydrogen atoms (Table 4S, 1 page); observed and calculated structure factors (Table 5S, 25 pages) are available from the authors on request.

Acknowledgements

We are grateful to Mr D. Bernardeschi for the preparation of the complexes, to the 'Ministero dell'Università e della Ricerca Scientifica e Tecnologica' (MURST) of Italy for grants, to the 'Centro Interdipartimentale Grandi Strumenti' of Modena University for X-rays data collection, and to the 'Centro Interdipartimentale di Calcolo Automatico ed Informatica Applicata' (CICAIA) of Modena University for computer facilities.

References

1 R. West (ed.), *Oxocarbons*, Academic Press, New York, 1980.
2 F. Serratosa, *Acc Chem Res*, *16* (1983) 170.
3 R. West and H Y. Niu, *J. Am. Chem. Soc.*, *85* (1963) 2589.
4 J.P. Chesick and F. Doany, *Acta Crystallogr*, *Sect. B, 37* (1981) 1076.
5 A. Weiss, E. Riegler and C. Robl, *Z Naturforsch., Teil B, 41* (1986) 1329.
6 A. Weiss. E. Riegler and C. Robl, *Z Naturforsch., Teil B, 41* (1986) 1333.
7 F. Lloret, M Julve, J. Faus, X. Solans, Y. Journaux and I. Morgenstern-Badarau, *Inorg. Chem., 29* (1990) 2232.
8 R. Soules, F. Dahan, J.P. Laurent and P. Castan, *J Chem Soc*, *Dalton Trans*, (1988) 587.
9 J.A.C. Van Ooijen, J. Reedijk and A.L. Spek, *Inorg. Chem*, *18* (1979) 1184.
10 M. Habenschuss and B.C. Gerstein, *J. Chem. Phys., 61* (1974) 852.
11 X. Solans, M. Aguilò, A. Gleizes, J. Faus, M. Julve and M. Verdaguer, *Inorg. Chem., 29* (1990) 775.
12 I. Castro, J. Faus, M. Julve, Y. Journeaux and J. Sletten, *J. Chem. Soc*, *Dalton Trans.*, (1991) 2533.
13 M Benetó, L. Soto, J. Garcia-Lozano, E. Escrivá, J.P. Legros and F. Dahan, *J. Chem. Soc., Dalton Trans*, (1991) 1057.
14 I. Castro, J. Faus, M. Julve, M. Verdaguer, A. Mongue and E. Gutierrez-Puebla, *Inorg. Chim Acta, 170* (1990) 251.
15 G Bernardinelli, D. Deguenon, R. Soules and P. Castan, *Can J Chem*, *67* (1989) 1158.
16 Q. Chen, S Liu and J. Zubieta, *Angew. Chem*, *Int Ed. Engl., 29* (1990) 70.
17 Q. Chen, L. Ma, S. Liu and J. Zubieta, *J. Am. Chem Soc*, *111* (1989) 5944.
18 Q. Chen, S. Liu and J. Zubieta, *Inorg Chim. Acta, 164* (1989) 115.
19 R. Soules, A. Mosset, J P. Laurent, P. Castan, G. Bernardinelli and M. Delamar, *Inorg Chim Acta, 155* (1989) 105.
20 G Bernardinelli, P. Castan and R Soules, *Inorg Chim Acta, 120* (1986) 205
21 O. Simonsen and H. Toftlund, *Inorg. Chem., 20* (1981) 4044.
22 J.C. Trombe, J.F. Petit and A. Gleizes, *New J. Chem*, *12* (1988) 197.
23 R West and H.Y. Niu, *J Am. Chem. Soc*, *85* (1963) 2586.
24 M.D. Glick and L F. Dahl, *Inorg. Chem*, *5* (1966) 289.
25 D. Deguenon, G. Bernardinelli, J P. Tuchagues and P Castan, *Inorg. Chem*, *29* (1990) 3031.
26 M.D. Glick, G.L. Downs and L.F. Dahl, *Inorg. Chem., 3* (1964) 1712.
27 I. Castro, J. Sletten, J. Faus, M. Julve, Y. Journaux, F. Lloret and S. Alvarez, *Inorg Chem*, *31* (1992) 1989.
28 I. Castro, J. Sletten, J. Faus and M. Julve, *J Chem. Soc., Dalton Trans.*, (1992) 2271
29 M. Aguilò, X Solans, I. Castro, J. Faus and M. Julve, *Acta Crystallogr*, *Sect. C, 48* (1992) 802.
30 Q. Chen, S. Liu and J. Zubieta, *Inorg Chim Acta, 175* (1990) 241.
31 C. Brouca-Cabarrecq and J C. Trombe, *Inorg Chim. Acta, 191* (1992) 227.
32 C Brouca-Cabarrecq and J.C. Trombe, *Inorg Chim Acta, 191* (1992) 241.
33 A.C.T. North, D C. Phillips and F.S. Mathews, *Acta Crystallogr., Sect A, 24* (1968) 351.
34 *International Tables for X-Ray Crystallography*, Vol. 4, Kynoch, Birmingham, UK, 1974, pp. 174–175.
35 G.M Sheldrick, *SHELX 76*, program for crystal structure determination, University Chemical Laboratory, Cambridge, UK, 1976.
36 C.K. Johnson, *ORTEP, Rep ORNL-3794*, Oak Ridge National Laboratory, Oak Ridge, TN, 1965.

37 A. Bencini and D. Gatteschi, *EPR of Exchange Coupled Systems*, Springer, Berlin, 1990.
38 A. Bencini and D. Gatteschi, *Transition Met Chem.*, *8* (1982) 1.
39 E. König, V.P Desai, B. Kanellakopulos and R. Klenze, *Chem. Phys.*, *54* (1980) 109.
40 M.E. Fisher, *Am. J. Phys*, *32* (1964) 343.
41 Y. Pei, M. Verdaguer, O. Kahn, J. Sletten and J.P. Renard, *Inorg. Chem*, *26* (1987) 138.
42 E. Coronado, M. Drillon, P R. Nutgeren, L J. deJongh, D. Beltran and R. Georges, *J Am Chem Soc.*, *111* (1989) 3874
43 P M. Richards, *Phys Rev*, *B, 10* (1984) 4687.
44 E Coronado, M Drillon, A. Fuertes, D. Beltran, A. Mosset and J. Galy, *J Am. Chem Soc*, *108* (1986) 900.
45 J C. Bonner and M E. Fisher, *Phys Rev*, *35* (1964) 640.
46 R.L. Carlin, *Magnetochemistry*, Springer, New York, 1986.
47 Y V. Rakitin, V.T. Kalinnikov and M.V. Eremin, *Theor. Chim Acta, 45* (1977) 167.